Beam density fluctuation diagnostic

W. W. Heidbrink[a)]

GA Technologies Inc., San Diego, California 92138

(Received 25 March 1988; accepted for publication 15 May 1988)

The conceptual design of a neutral particle analyzer that is optimized for spatially resolved fluctuation measurements is described. Estimates indicate that a pair of these analyzers could detect fluctuations in beam-ion density associated with high β instabilities in the DIII–D tokamak.

INTRODUCTION

Charge-exchange diagnostics have generally focused on measurements of the energy distribution of escaping neutrals. Spectral measurements have proven invaluable during ion wave heating where, *a priori*, the ion distribution is completely unknown. During neutral beam heating, the suprathermal distribution is usually determined primarily by the beam orientation and injection voltage, so the role of spectral measurements, generally, is to detect deviations from classical behavior. Many detailed comparisons between experiment and theory have been performed and rough agreement with classical theory has generally been obtained.[1] The uncertainties in modeling the charge-exchange spectrum are sufficiently large, however, that discrepancies as large as a factor of 2 are considered compatible with theory. Only during severe losses of beam ions, as during the fishbone instability in PDX,[2] have clear deviations from classical behavior been identified in the slowing-down spectrum.

Under some conditions, impulsive transport of beam ions at MHD bursts is evidenced by a sudden increase in neutral flux.[2–4] Many plasma instabilities are virtually continuous, however, so any beam-ion transport associated with these instabilities cannot readily be identified from the time evolution of the flux. How can steady transport that does not strongly distort the spectrum be identified? One approach is to study quantitatively the beam density profile using active charge exchange. Another approach, considered here, is to measure directly fluctuations in beam density $\tilde{n}_b$ in a localized volume of the plasma. Although knowledge of $\tilde{n}_b$ alone does not suffice to calculate transport, the dependence of $\tilde{n}_b$ on plasma conditions could yield important insights into beam-ion behavior.

Section I discusses, conceptually, the design of a neutral particle detector that is optimized for spatially resolved flux measurements. Section II discusses the use of a pair of these detectors on DIII–D. Spatial localization of the $\tilde{n}_b$ measurement is obtained by studying the coherence of a pair of detectors that have intersecting sightlines in the plasma. The technique has poorer wavelength resolution than conventional electron density fluctuation measurements. Its merit is that beam density fluctuations differ from electron density fluctuations for many instabilities.

I. NEUTRAL FLUX DETECTOR

The design of the flux detector is based on the minianalyzer used in studies of the fishbone instability[3,5] but with further modifications to enhance temporal resolution at the expense of energy resolution. The instrument consists of a collimator, a stripping foil, electrostatic deflection plates, and a channel electron multiplier (CEM) housed inside a soft iron shield (Fig. 1). The principal considerations in the design of the detector are the spatial resolution and the signal level.

Spatial resolution is obtained primarily by collimation of the incident neutrals. Realistic geometries for DIII–D are discussed in the next section but, for an initial estimate, the spatial resolution Δx is roughly

$$\Delta x \simeq r\Delta\varphi, \tag{1}$$

where $\Delta\varphi (\ll 1)$ is the angular acceptance of the collimator in the plane of interest and r is the distance between the detector and the emitting plasma volume. The simplest form of collimation is obtained using fixed baffles separated by a distance d. Unfortunately, the collimation provided by baffles of area A is roughly $\Delta\varphi \simeq \sqrt{A}/d$ so, for good collimation such that the cross-sectional area $(\Delta x)^2$ of the viewed volume is nearly as small as the area of the detector, the distance between the entrance aperture and the detector must be inconveniently large ($d \simeq r$). These considerations dictate the use of a collimating element with narrow collimation but large effective area.

The goal of the design is to maximize the detected signal Φ without sacrificing spatial resolution in the plasma. The signal from a volume V is

$$\Phi \simeq SV(A_d/4\pi r^2)\eta_c\eta_f\eta_E\eta_d, \tag{2}$$

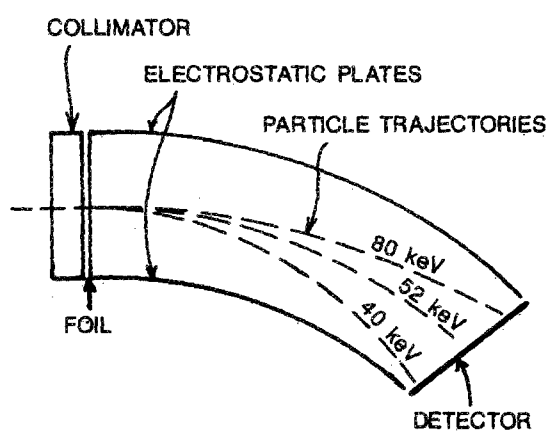

FIG. 1. Sketch of a neutral flux detector.

 0034-6748/88/092008-04$01.30

where S is the neutral emissivity from the volume, A_d is the area of the detector, η_c is the transmission of the collimator, η_f is the fraction of incident neutrals transmitted and ionized by the foil, η_E is the fraction of incident neutrals within the energy range selected by the electrostatic plates, and η_d is the efficiency of detection of the CEM. Equation (2) assumes isotropic neutral emission from the plasma which is, of course, an invalid assumption; nevertheless, Eq. (2) is helpful in identifying factors that enhance the signal Φ. Physics requirements (Sec. II) dictate that the volume V be as small as possible. To maximize the signal and minimize the volume at fixed collimation, the distance r between the plasma volume and the instrument should be as small as possible. This dictates that the instrument be compact and well shielded so that it can be mounted close to the tokamak vacuum vessel. To maximize the signal without significantly degrading the spatial resolution, the area of the detector should be of roughly the same linear dimension as the viewed volume, i.e., $A_d \simeq V^{2/3}$. The transmission of the collimator η_c should be as large as possible, the stripping foil should ionize a large fraction of incoming neutrals ($\eta_f \lesssim 50\%$),[6] and the detector should collect all incident ions ($\eta_d \simeq 1$). Specification of the energy resolution (which determines η_E) is more subtle. From the standpoint of temporal resolution, it is desirable to collect neutrals of all energies ($\eta_E \rightarrow 1$). However, beam ions of all energies may not respond identically to instabilities, so some energy discrimination is desirable.

These considerations give rise to the design sketched in Fig. 1. The collimator is fabricated from leaded glass using the technology developed for fiber optics and microchannel plates. Physically, the plate must be sufficiently thick that incident 80-keV neutrals cannot burrow through the walls but must travel down the channels. The range of a 100-keV proton in lead is less than 1 μm so, in practice, the plate can be any convenient thickness (e.g., 1 mm). Good collimation is desirable so 100:1 channels are employed. Use of an amorphous material eliminates channeling, which otherwise could limit the effective collimation. The diameter of the collimator is 1 cm. The collimator is placed before the stripping foil because neutrals are easier to collimate than ions (no stray field effects). The ratio of channel area to total area is approximately $\eta_c \simeq 0.6$.

The stripping foil is a thin layer of carbon supported on a 90% transparent nickel mesh. To minimize energy loss and straggling, the foil should be thin but it need not be as thin as in previous work[3,5] since the energy resolution of the instrument is already relatively poor. A foil 1 cm in diameter and 10 μg/cm^2 ($\sim$400 Å) thick is practical.

The energy resolution afforded by the electrostatic plates is very coarse. The primary role of the plates is to deflect the ions so that x rays that penetrate the collimator and foil cannot reach the detector without first reflecting off the (blackened) walls. Only a 35° bend is employed so that a large energy band is simultaneously collected. Because of the relatively large separation between plates, the bias voltage is rather large [$V_{\text{bias}} = E \ln(b/a)/Z \simeq 7.8$ keV for $E/Z = 50$ keV] but the dielectric strength of the vacuum is adequate to avoid breakdown.

The ions are detected by a CEM with 1-cm-diam active area. The detector is operated in the current mode.

The whole assembly is housed in a thick (e.g., 1 in.), compact ($\sim 9 \times 9 \times 9$ in.), soft iron shield.

II. APPLICATION IN DIII-D

A single detector integrates the flux emitted anywhere along its sightline. To obtain spatial resolution, a pair of detectors with intersecting sightlines are employed (Fig. 2). The intersection volume is arranged to lie within the path of one of the heating beams, which provides a local source of neutrals in the plasma. (Otherwise, the signal is dominated by the high neutral density region at the plasma edge.) The intersection volume is situated in the outer part of the plasma to minimize the effect of neutral attenuation on the doping beam and the exiting neutrals, and because the predicted amplitude of pressure-driven modes peaks in this region. The arrangement of diagnostic ports on DIII-D suggests several possible configurations for the measurement; in perhaps the best configuration, detectors are placed in adjacent ports in the horizontal midplane (Fig. 2). This configuration has the advantage of placing the detectors close to the plasma volume and of viewing neutrals near the angle of beam injection, both of which tend to enhance the signal level. The configuration is also conducive to radial variation of the intersection volume. Its disadvantage is that the sightlines do not intersect at right angles, so the length of the viewing volume is increased by a factor of 4 over the mini-

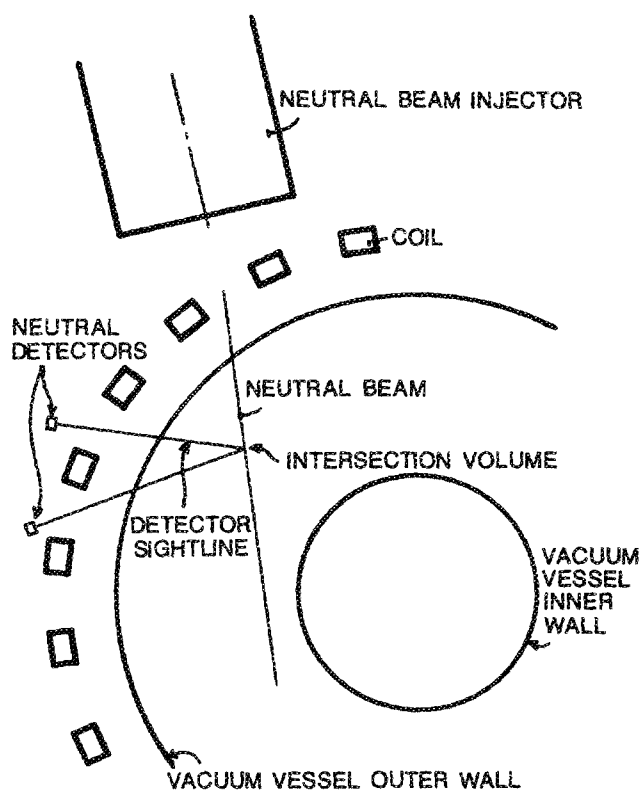

FIG. 2. Plan view of DIII-D showing the layout of a beam density fluctuation diagnostic.

mum possible value. Two other possible configurations also merit consideration. The detectors could be separated by two field coils in the horizontal midplane, which gives substantially better spatial resolution since the sightlines intersect at right angles. A difficulty with this configuration is that one detector views circulating particles while the other views trapped particles. Conceivably, these two classes of beam ions might respond differently to an instability. A third possible configuration is a vertically viewing detector crossed with a horizontal detector. Because of the elongation of the DIII–D vacuum vessel, the improvement in spatial resolution associated with a crossed viewing geometry is partially offset by the larger path length r [compare Eq. (1)] so that the spatial resolution is only improved by a factor of 2. Relative to detectors in the midplane, a disadvantage of this configuration is that the detector is twice as far from the intersection volume so the signal is reduced a factor of 4. The reduction is even greater at higher densities ($\bar{n}_e \gtrsim 4\times 10^{13}$ cm^{-3}), where attenuation of the escaping neutrals becomes important.

Fluctuations in beam density in a localized volume are obtained through cross-spectral analysis of the two signals.[7] Fluctuations from the intersection volume result in fluctuations in signal that are coherent and in phase; instabilities from other regions of the plasma are assumed to make negligible contributions to the coherency spectrum due to phase mixing. Actually, of course, coherent oscillations in signal can be produced by instabilities with long wavelengths; in fact, large coherent oscillations were observed with two separated neutral particle detectors during the fishbone instability in PDX.[3] Experimentally, the contribution of fluctuations outside of the intersection volume can be assessed through two techniques. One test is to turn off the heating beam used as a local source of neutrals. If the features in the spectrum persist, they are probably due to a long-wavelength edge instability. Edge oscillations may also exhibit a phase lag, which could be identified by deviations from 0° in the phase spectrum. A second test is to tilt the sightline of one of the analyzers away from the horizontal midplane: the coherency should decrease with increasing distance. This technique could also help establish the scale length of detected fluctuations.

A rough estimate indicates that the signal level is sufficient for measurements at 1 MHz. In the outer region of the plasma (before appreciable attenuation through ionization) the neutral density in a heating beam is $n_0 \simeq 10^9$ cm^{-3}. In a moderate-density L-mode plasma at full power (10 MW), the density of beam ions above $E_{\rm inj}/2$ is $n_b \sim \dot{N}_b \tau_s / V_p \sim 5\times 10^{11}$ cm^{-3}, where $\dot{N}_b$ is the injection rate, τ_s is the slowing-down time, and V_p is the plasma volume. The emissivity of 40–80-keV neutrals from the intersection volume is $S = n_0 n_b \langle \sigma v \rangle \sim 2\times 10^{13}$ cm^{-3} s^{-1}. The emission is anisotropic in pitch angle and some emitted neutrals reionize. Assume that the detectors are oriented to view a heavily populated pitch angle (as in Fig. 2) and that reionization is small (i.e., $\bar{n}_e \lesssim 7\times 10^{13}$ cm^{-3}). For the configuration illustrated in Fig. 2 with the detectors described in Sec. I, the intersection volume is approximately $1.5\times 1.5\times 7$ cm. Using Eq. (2), the expected signal is $\Phi \sim 10^8$ cps. This large signal level implies that high-frequency (1 MHz) measurements of 1% fluctuation are not limited by counting statistics for reasonable time records (e.g., 10 ms). Since the neutral density n_0 depends on the attenuation of the injected beam along the whole beam trajectory, it is expected to fluctuate weakly in response to instabilities with wavelengths $\lambda \ll a$ (a is the plasma minor radius). Thus fluctuations in signal are due primarily to fluctuations in beam density $\tilde{n}_b$.

Although the temporal resolution of the $\tilde{n}_b$ measurement is good, the ability to resolve small-scale structure is poor when compared to conventional wave-scattering techniques such as CO_2 or microwave scattering. In one sense, the spatial resolution of a CO_2 laser scattering experiment is rather poor since the scattered light is typically collected from a very large volume. But since the scattered waves are constrained by the Manley–Rowe relations, $k_i - k_s = \pm k_0$, the wavelength of the detected fluctuations is known accurately. In contrast, when collecting particles emitted from a volume, phase mixing tends to obscure fine-scale fluctuations so that the wavelength resolution is approximately the length of the volume.

Ballooning modes are thought by many to be responsible for the beta limit in tokamaks.[8] These modes have small radial wavelengths and are purely growing in ideal MHD. The high n modes tend to be destabilized first, although lower n modes usually have similar stability properties. Another class of instabilities postulated to affect transport in tokamaks are the various drift instabilities.[9] A typical frequency for these modes is the diamagnetic drift frequency and a typical perpendicular wavelength is the (thermal) ion gyroradius.

Although the frequency response of the neutral flux detectors is sufficient to detect high n ballooning modes and drift waves, the spatial resolution is not. On the other hand, modes with a ballooninglike structure with $n < 10$ have been observed at high beta on several tokamaks.[10] Furthermore, in studies of the nonlinear saturation of ballooning modes,[11] longer wavelength harmonics have the greatest effect on transport. The effect of these or similar modes on beam density fluctuations could be detected with the proposed diagnostic.

The plasma maintains quasineutrality for all low-frequency modes. Naively, this suggests that measurements of $\tilde{n}_b$ are equivalent to electron density fluctuation ($\tilde{n}_e$) measurements. Because of the large banana width of hot ions, however, the beam ions respond differently to instabilities than electrons. Charge neutrality is preserved by fluctuations in the "third" species, the thermal ions. Besides their gyroradius, there is another important difference between beam ions and electrons. In most plasmas, the gradient in beam density is much steeper than the electron density gradient, which also tends to make $\tilde{n}_b/n_b \neq \tilde{n}_e/n_e$. Recent theoretical studies[12] have found that the unique dynamics of a hot species modifies the behavior of several well-known instabilities.

In conclusion, detection of steady-state transport of beam ions using conventional charge-exchange techniques is difficult. Neutral detectors optimized for high count rates can detect fluctuations in beam density associated with low n

($\lesssim 10$), ballooninglike instabilities. The information available from these measurements complements conventional electron fluctuation measurements.

ACKNOWLEDGMENTS

The author thanks K. H. Burrell, R. R. Dominguez, J. Lovberg, R. D. Stambaugh, and A. H. Turnbull for helpful discussions. This work was supported by the U.S. Department of Energy under Contract No. DE-AC03-84ER51044.

[a] Present address: University of California, Irvine, California 92717.

[1] R. Kaita, R. J. Goldston, P. Beiersdorfer, D. L. Herndon, S. M. Kaye, H. W. Kugel, R. T. McCann, D. C. McCune, D. D. Meyerhofer, and H. H. Towner, Nucl. Fusion **25**, 939 (1985) and references therein.

[2] K. McGuire *et al.*, Phys. Rev. Lett. **50**, 891 (1983); R. J. Goldston *et al.*, Nucl. Fusion **27**, 921 (1987).

[3] P. Beiersdorfer, R. Kaita, and R. J. Goldston, Nucl. Fusion **24**, 487 (1984).

[4] W. W. Heidbrink *et al.*, Phys. Rev. Lett. **57**, 835 (1986); W. W. Heidbrink *et al.*, Phys. Fluids **30**, 1839 (1987).

[5] P. Beiersdorfer, A. L. Roquemore, and R. Kaita, Rev. Sci. Instrum. **58**, 2092 (1987).

[6] J. A. Phillips, Phys. Rev. **97**, 404 (1955).

[7] G. M. Jenkins and D. G. Watts, *Spectral Analysis and its Applications* (Holden-Day, San Francisco, 1968), Chaps. 8 and 9.

[8] For example, W. H. Choe and J. P. Friedberg, Phys. Fluids **29**, 1766 (1986), and references therein.

[9] For example, R. R. Dominguez and R. E. Waltz, Nucl. Fusion **27**, 65 (1987); W. M. Tang, Nucl. Fusion **26**, 1605 (1986).

[10] K. M. McGuire, Princeton Plasma Physics Laboratory Rep. PPPL-2134 and references therein.

[11] M. Hossain and H. R. Strauss, Bull. Am. Phys. Soc. **32**, 1919 (1987).

[12] For example, H. Biglari and L. Chen, Phys. Fluids **29**, 2960 (1986).